Asian Journal of Applied Science and Technology (AJAST)
Volume 6, Issue 3, Pages 25-34, July-September 2022

Biocompatible Molybdenum Complexes Based on Terephthalic Acid and Derived from PET: Synthesis and Characterization

Cesar E. Castañeda-Calzoncit[1], Denis A. Cabrera-Munguia[1*], Jesús A. Claudio-Rizo[1], Dora A. Solís-Casados[2] & Claudia M. López-Badillo[3]

[1]*Materiales Avanzados, Facultad de Ciencias Químicas, Universidad Autónoma de Coahuila, Blvd. Venustiano Carranza 935, República, 25280 Saltillo, Coahuila, México. Email: dcabrera@uadec.edu.mx**
[2]*Centro Conjunto de Investigación en Química Sustentable, UAEM-UNAM, carr. km 14.5 unidad San Cayetano Toluca-Atlacomulco, Toluca, Estado de México, México.*
[3]*Materiales Cerámicos, Facultad de Ciencias Químicas, Universidad Autónoma de Coahuila, Blvd. Venustiano Carranza 935, República, 25280 Saltillo, Coahuila, México.*

DOI: http://doi.org/10.38177/ajast.2022.6304

Article Received: 22 May 2022 *Article Accepted: 24 July 2022* *Article Published: 16 August 2022*

ABSTRACT

Metal-organic molybdenum complexes were synthesized by the hydrothermal method using ammonium heptamolybdate as the metallic source, and as the organic ligand terephthalic acid (BDC) or bis(2-hydroxyethyl) terephthalate (BHET), obtained via glycolysis of poly(ethylene)terephthalate (PET). The BDC-Mo and BHET-Mo complexes were characterized by XRD, N_2 physisorption, TGA, ATR-FTIR, SEM, XPS and their *in vitro* biocompatibility was tested by porcine fibroblasts viability. The results show that molybdates (MoO_4^{-2}) are coordinated to the carbonyl functional groups of BDC and BHET by urea bonding (-NH-CO-NH-) which is related to their high biocompatibility and high thermal stability. These organic molybdate complexes possess rectangular prism particles made up of rods arrays characteristics of molybdenum oxides (MoO_3). The organic complexes BDC-Mo and BHET-Mo do not show to be cytotoxic for porcine dermal fibroblasts growing on their surface for up to 48 h of culture.

Keywords: *Molybdenum complexes, Terephthalic acid, bis(2-hydroxyethyl) terephthalate, Cell viability, Biocompatibility.*

1. Introduction

Molybdenum (Mo) is the only transition metal from the second row of periodic table that is required for bacteria, plants, animal, and humans [1], since molybdenum takes part of the metabolism of carbon, nitrogen, and sulfur compounds, [2] and due to its abundance in the oceans in the form of the soluble molybdate ion (MoO_4^{-2}) is easily uptake by the living organisms [1, 2]. In the human body, Mo is a trace element that has acts as cofactor in the form of enzymes like xanthine oxidoreductase, mitochondrial amidoxime, aldehyde oxidase, and sulfide oxidase [3, 4]. However, to obtain biologic activity Mo must be complexed to protein compound to form molybdenum cofactor (Moco) [4].

On the other hand, organic ligands constituted by carboxylic groups are biocompatible, due to their great polarity they can be easily removed from animal by urine and feces [5]. Specifically, terephthalic acid (BDC) has been used in the construction of Metal-Organic Frameworks (MOFs), being a hard base mixed with hard acid such as Cr^{+3}, Al^{+3}, Fe^{+3}, and Zr^{+4} leading to the water stable MOF series MIL and UiO [6, 7].

Also, polyethylene terephthalate (PET) is a non-biodegradable polymer with high resistance to degradation by hydrolytic cleavage of chemical bonds, but it can be depolymerized by glycolysis obtaining as a main product bis(2-hydroxyethyl) terephthalate (BHET) using acid Lewis catalyst [8]. In a previous work, BDC and BHET were used as organic ligand to form coordination polymers with aluminum ion (Al^{+3}) obtaining outstanding biocompatible properties in the metabolism of fibroblast [9], also these compounds were used as active ingredients in the formulation of a gel based on collagen to heal skin chronic wounds such as burns, venous ulcer, and diabetic neuropathy [10].

In the present work, it is proposed the synthesis of two molybdenum complex based on ammonium heptamolybdate (AHM) and BDC or BHET as organic linker, where BHET was previously obtained from PET depolymerization. The hydrothermal process was employed as the synthesis method using water as a solvent to assure the biocompatibility of the compounds, avoiding traces of organic solvents. The crystal, textural, chemical structure, thermal stability and biocompatibility of BDC-Mo and BHET-Mo were systematically studied obtaining molybdenum-based complexes that crystalize in the form of rectangular prism composed of rods arrays, where fibroblast can live up to 48 h without affecting their metabolism, as it is shown in the fluorescence images with calcein (Fig.1), and thus these novel materials could be potential candidates for biomedical applications in tissue engineering and controlled drug delivery.

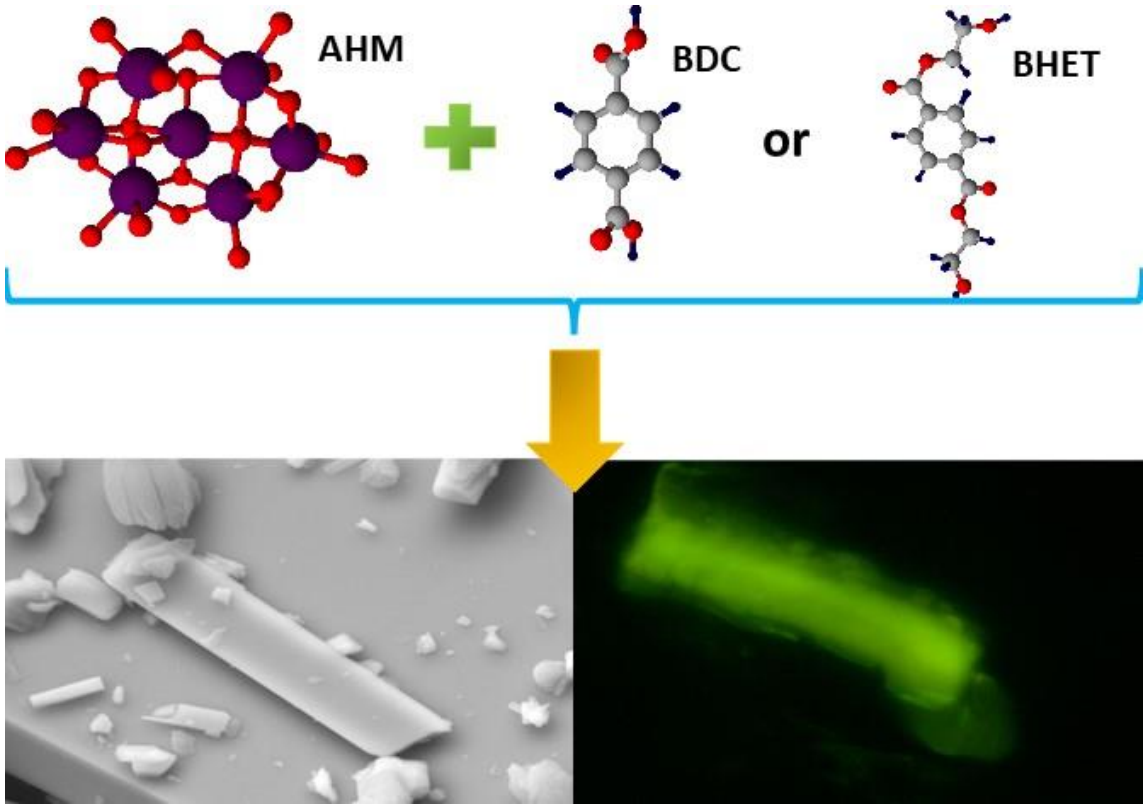

Fig.1. Synthesis of molybdenum complexes and fibroblast proliferation using Live/Dead assay

2. Methods

2.1. Synthesis of molybdenum complexes

The BDC-Mo and BHET-Mo complexes were synthesized mixing 5 mmol of ammonium heptamolybdate ($(NH_4)_6Mo_7O_{24}.4H_2O$, AHM) and 17.5 mmol of terephthalic acid ($HOOC\text{-}C_6H_4\text{-}COOH$, BDC) or 17.5 mmol of bis(2-hydroxyethyl) terephthalate ($HO\text{-}C_2H_4\text{-}OOC\text{-}C_6H_4\text{-}COO\text{-}C_2H_4\text{-}OH$, BHET), the latter was obtained previously by the depolymerization of PET bottles, the glycolysis procedure was described somewhere else [9]. The metallic precursor and the organic ligand were dissolved and mixed in 50 mL of distillated water, the solution was put into a Teflon-lined steel autoclave and heated up to 120ºC for 72 h. The hydrothermal reactor was opened containing a blue-colored suspension that was filtrated under vacuum, obtaining a whitish precipitate which was washed with distillated water, and it dried at 80ºC during 12 h.

2.2. Physicochemical characterization

The XRD diffractograms of BDC-Mo and BHET-Mo complexes as well as their precursors were acquired in a 2θ range from 5º to 40º with a Cu Kαx ray source (λ=1.540 Å) using a *SAXS-Emc2, Anton Paar* diffractometer. The infrared spectra of BDC-Mo and BHET-Mo materials were acquired with a resolution of 16 cm^{-1} from 4000 to 600 cm^{-1} using *Perkin Elmer Frontier* equipment.

The X-ray photoelectron analysis (XPS) of BDC-Mo and BHET-Mo was done employing a *JEOL photoelectron spectrometer* model *JPS-9200* equipped with a monochromatic Mg X-ray radiation (300 W, 15 kV and 1253.4 eV). The powders of materials were deposited on a conducting scotch tape and located in Al tapes on stainless steel sample holders, which remained in a pre-analysis chamber until a pressure of 10^{-3} mbar was achieved before entering the analysis chamber. Survey spectra were recorded from 0 to 1100 eV at constant pass energy of 100 eV, onto 900 μm^2 of analysis area; narrow spectra of C1s, O1s, N1s and Mo3d regions were recorded in the constant pass energy mode at 20 eV, dwell 100 and 10 scans at least, *Specsurf* version 1.8.2 was used for acquisition. Origin v.9.0 was used for data analysis, the charge correction was adjusted with carbon signal C1s 284 eV. A Shirley type background was subtracted as baseline from the spectra and signal was deconvoluted using Gaussian curves to determine binding energies of the different element core level. NIST database was used to identify the corresponding element of the measured binding energies.

The textural properties such as surface area and mean pore diameter of BDC-Mo and BHET-Mo complexes were analyzed by N_2 adsorption using the BET method. The nitrogen physisorption experiments were carried out in a *Quantachrome Autosorb iQ* instrument, with a previous outgassing of the samples at 200ºC during 12 h. The thermal properties of materials were measured in a *TGA-4000 Perkin Elmer* thermoanalyzer, where 5 mg of sample were heated since room temperature until 800ºC with a heating rate of 20ºC/min, and a N_2 flow of 20 mL/min as inert atmosphere. The SEM micrographs were acquired in a *JEOL JSM-6510LV* scanning electron microscope.

2.3. Analysis of in vitro biocompatibility

The viability of porcine fibroblasts growing on water suspensions of molybdate complexes was assessed. Fibroblasts suspension in DMEM culture medium was added to every well (50,000 cells) that contain every molybdenum complex in a water suspension and the control (phosphate buffer solution (PBS 1X)), these were incubated for 24 and 48 h. The cell viability was determined by the active metabolism of these cells to transform MTT salts into formazan with respect to control. The MTT (1% w/v) was added to wells with materials and controls, and afterward, the cells were kept up under culture conditions for 3 h at 37 °C. At that point, the medium was tapped, the blue formazan was diluted in isopropanol, and the absorbance of the solutions was estimated at 560 nm, using a *Thermo Scientific Multiskan Sky* spectrophotometer. The absorbance of generated formazan by cells growing in the control (PBS 1X) is equal to 100% of viability, thus the cell viability ratio was calculated dividing the obtained absorbance by complex water suspension between the control absorbance.

3. Results and Discussion

Fig.2a shows the diffractograms of BHET, $(NH_4)_6Mo_7O_{24}.4H_2O$ and BDC. The BDC sample exhibits the peaks 17.3°, 25.1°, and 27.8° at 2θ that correspond to the double hydrogen bonded molecular chains of BDC leading to

the form of plates and needles [11]. While the XRD of BHET shows characteristic signals at 2θ=10.2°, 16.3°, 21.1°, 23.3°, and 27.4° typical of crystals in the form of needles [12]. The XRD pattern indicates intense signals at 2θ=11.9°, 12.2° and 12.60° which are in line with the ICDD PDF card 21-0571 related to molybdenum oxide ammonia hydrate confirming the crystal structure of ammonium heptamolybdate.

Fig.2b depicts the XRD patterns of BDC-Mo and BHET-Mo, most of the characteristic peaks are associated to the crystal structure of ammonium tetramolybdate ($(NH_4)_2Mo_4O_{13,}$ ICDD PDF card 80-0756) with intense signals at 2θ= 12.3°, 13.7°, 14.7°, 25.6°, 26.9° y 30.4° related to the planes (0 2 1), (1 1 1), (0 2 2), (2 1 2), (0 4 3), and (1 0 6), respectively [13]. The characteristic diffraction peaks of BDC with a smooth left shift of 0.1° appear in both BDC-Mo and BHET-Mo indicating the coordination bonding between the ligand and molybdenum octahedrons. Also, small peaks at 11.3°, 18.9°, 21.8°, and 23.5° indicate the presence of the biuret crystal phase ($NH(CONH_2)_2$) [14]. In addition, the crystal data of both BDC-Mo and BHET-Mo is provided in Table 1, these data were obtained with the software *FullProof Suite ToolBar* using *DicVol04 tool* by selecting the 20 most intense peaks, it was obtained that Mo-BDC and Mo-BHET possess a monoclinic crystal system typical of molybdenum complexes [15, 16] with a space group P 2/m.

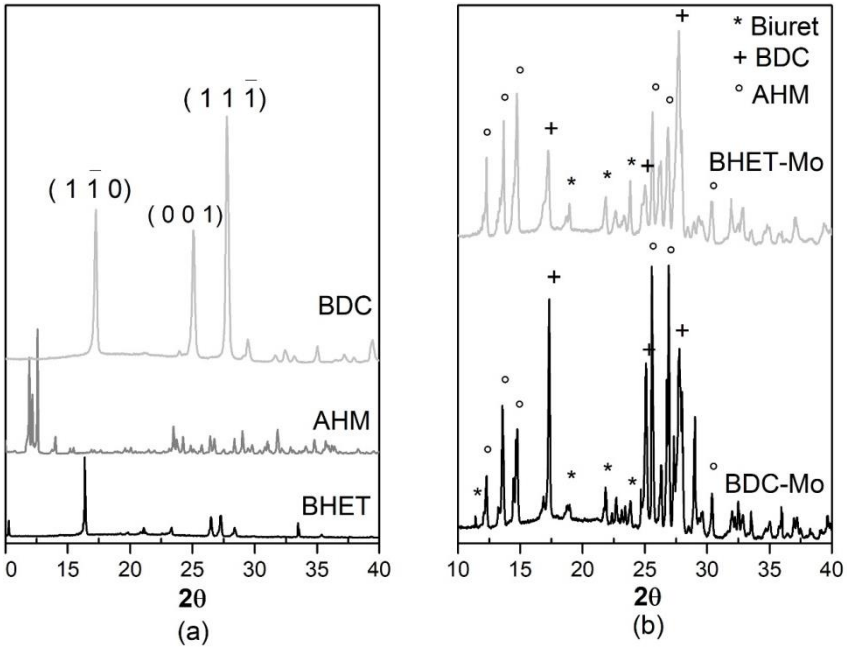

Fig. 2. XRD patterns of (a) precursors and (b) molybdenum complexes

Table 1. Crystal data and textural properties of molybdenum complexes

PROPERTY	BDC-MO	BHET-MO
Crystal system	Monoclinic	Monoclinic
Space group	P 2/m	P 2/m
a (Å)	19.2875	13.7498
b (Å)	15.3559	14.3278

c (Å)	7.8349	10.6793
α (°)	90	90
β (°)	91.17	107.01
γ (°)	90	90
Volume ($Å^3$)	2320.02	2011.80
BET surface area (m^2/g)	1.592	2.486
BJH pore diameter (nm)	1.716	1.388
Pore volumen (cm^3/g)	0.003	0.008

The SEM images of BDC-Mo and BHET-Mo are shown in Fig.3 evidencing that molybdenum complexes present rectangular prism particles which are typical of molybdenum oxides (MoO_3) generating rods arrays [17], and other complexes based on molybdenum and imidazole as ligand [18, 19]. The only difference between BDC-Mo and BHET-Mo is that the rectangular prism particles are more flattened in BHET-Mo than in BDC-Mo, thus obtaining more rods arrays in BHET-Mo, this correlates with the cell angles calculated (Table 1).These results also imply the major surface area and volume pore for BHET-Mo in comparison with BDC-Mo, however BDC-Mo shows a slightly greater pore diameter than BHET-Mo, this being typical for microporous materials (Table 1).

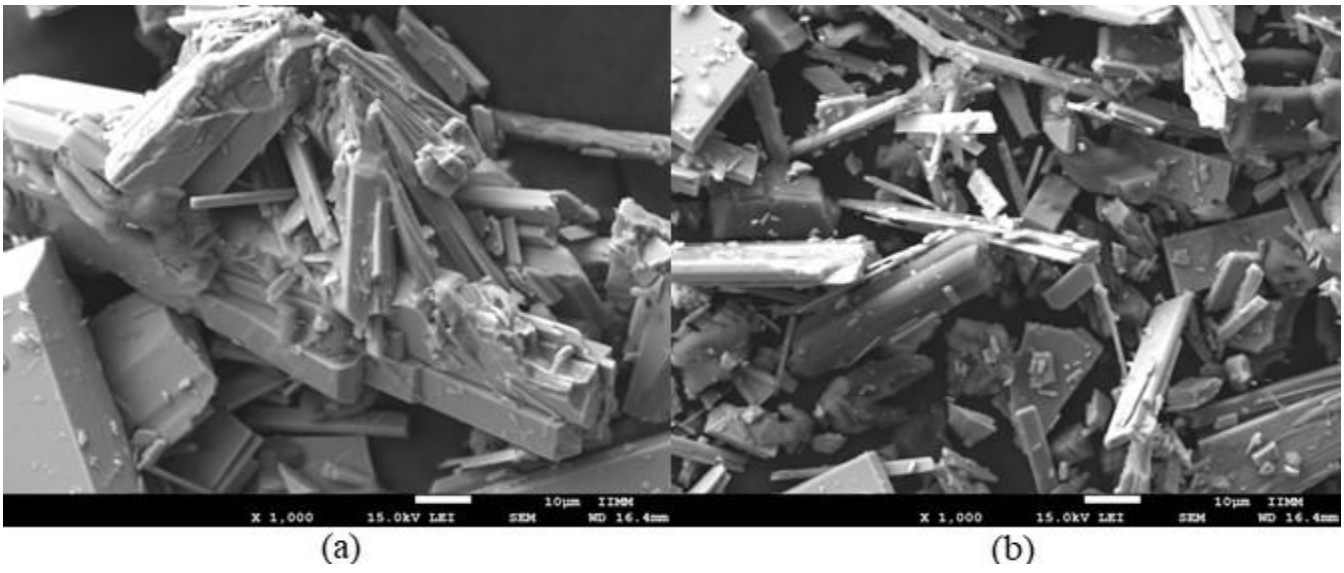

Fig.3. SEM micrographs of (a) BDC-Mo and (b) BHET-Mo

The ATR-FTIR spectra of the BDC and BHET precursors are shown in Fig.4a. Both precursors exhibit similar bands at 3200-3000 cm^{-1}, 1570 cm^{-1}, and 1400 cm^{-1} that are related to the C-H bonds and the C-C stretching vibrations of the benzene ring [14, 20]. Also, there are two bands at 1280 cm^{-1} and 1720 cm^{-1} associated to the vibration of C=O of the acyl group [14, 20]. The BDC shows an additional broad band at 940 cm^{-1} that belongs to the bending vibration of -OH bond from the carboxyl group [14]; while BHET depicts additional bands at 1450 cm^{-1} and 3430 cm^{-1} that correspond to methylene bonds ($-CH_2$) and hydroxyl bonds (-OH), respectively [20].

Fig.4b plots the FTIR spectra of BDC-Mo and BHET-Mo complexes which are very similar. Both spectra indicate broad bands (2900-3300 cm^{-1}) related to the stretching region of N-H and O-H bonds [14]. The band at 1720 cm^{-1} from BDC and BHET suffers a small shift to lower wavenumber at 1680 cm^{-1} obtaining a broad band, indicating the carbonyl stretching in molecules containing the NH-CO-NH group, this shift is attributed to the coordination through the oxygen atom with a metal to form complexes [14], this implies that carboxylic groups of BDC and BHET ligands are losing hydroxyl groups forming coordination bonds, which explains the loss of the characteristic band of hydroxyl groups of BHET in BHET-Mo complex. Also, the bending vibrations of the C=O bonds are found as small bands at 630 cm^{-1} and 675 cm^{-1} evidencing that the coordination bonding in BDC-Mo and BHET-Mo is mainly formed between molybdenum ions and carbonyl groups of BDC and BHET ligands [14]. In addition, the bands at 1570 cm^{-1}, 1400 cm^{-1} and 1280 cm^{-1} are attributed to the C-H bonds, C-C stretching vibrations of the benzene ring, and the vibration of the C=O of the acyl group. The bands at 884 cm^{-1} and 739 cm^{-1} represent the stretching vibration of the Mo=O terminal group, and to the flexural vibration of the Mo-O-Mo group, respectively [13].

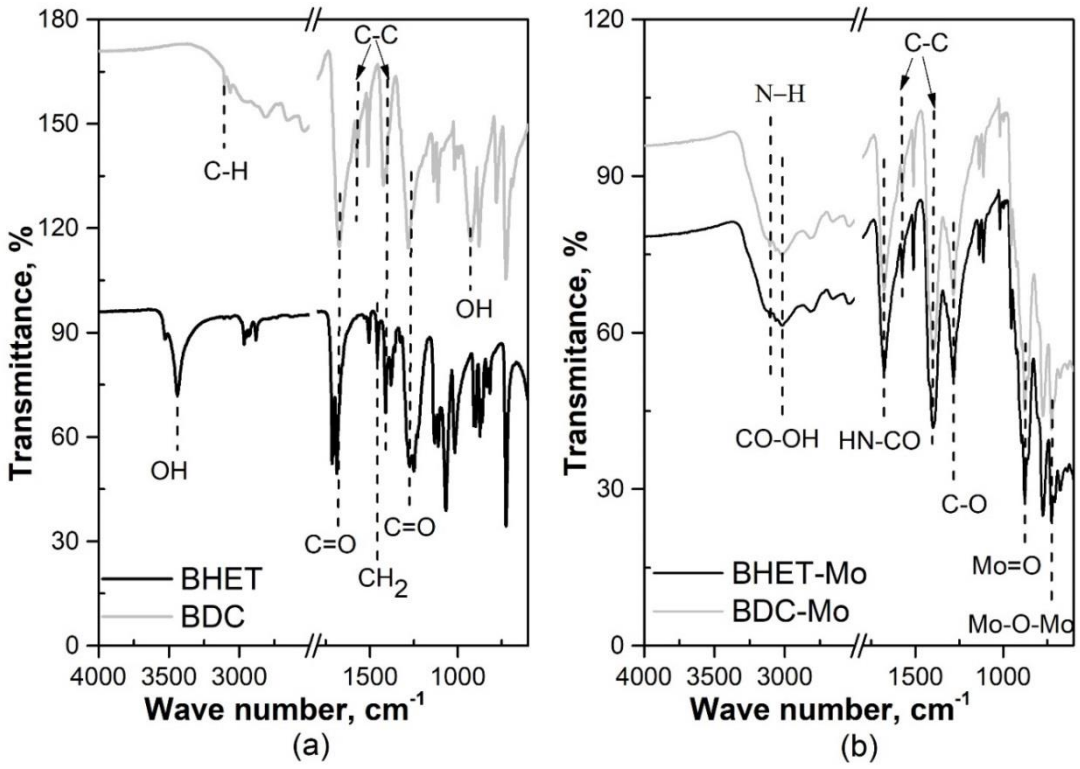

Fig.4. ATR-FTIR spectra of (a) precursors and (b) molybdenum complexes

Fig.5 depicts the high resolution XPS spectrum of O1s of molybdenum complexes with their corresponding deconvolution peaks. Both materials show deconvolution bands with similar binding energies, but BHET-Mo shows and additional deconvolution peak to the three peaks obtained for BDC-Mo.

The first band for both materials centered in a binding energy of 530.2-530.3 eV that according to the XPS NIST data base correspond to oxygen bonded to molybdenum as molybdate groups (MoO_4^{-2}). The second peak centered in a binding energy of 531.3-531.7 eV is attributed to oxygen in compounds based on urea bonding (-NHCONH) like the one found in biuret molecule ($HN(CONH_2)_2$). The third peak centered in a binding energy of 532.3-532.9

eV is related to the oxygen of carbonyl groups attached to the benzene ring (-O=C-C_6H_5). While the additional peak presented in the BHET-Mo complex at ~533.4 eV indicates the oxygen nearing the carboxyl groups related to the ester bonds of the BHET linker which is in line with the results found in FTIR spectra.

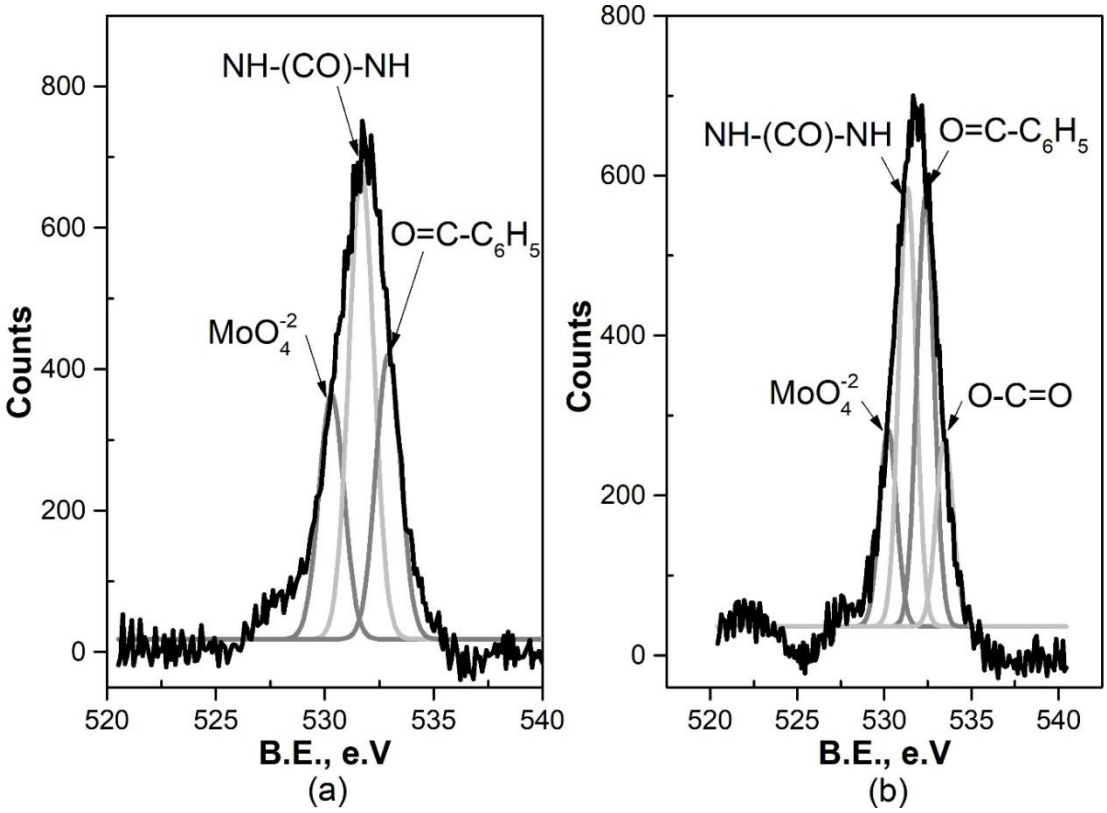

Fig.5. XPS narrow spectra of O1s (a) BDC-Mo and (b) BHET-Mo

The thermogravimetric analysis of BDC-Mo and BHET-Mo are plotted in Fig.6a. The TGA plot for both materials depicts a sharp weight loss between 32% to 35% for BHET-Mo and BDC-Mo, respectively, in a range temperature of 300°C-375°C that is associated to the loss of ammonium ions bonded to molybdate groups [21] and the decomposition of BDC and BHET ligands. However, the trace thermal degradation of ligands continues up to 543°C and 610°C for BDC-Mo and BHET-Mo complexes [22] leading to molybdenum oxides. BHET-Mo shows higher resistance to endothermic decomposition. indicating that the nucleophilic hydroxyl groups in BHET improve the structural stability of this molybdenum-based complex.

The biocompatibility of molybdenum complexes was analyzed with a fibroblast viability assay at 24 h and 48 h (Fig.6b). The results of fibroblast viability probe indicate that both BDC-Mo and BHET-Mo materials exhibit an enhanced cell viability higher than the control (PBS 1X). It is expected that the end carboxyl groups of BDC guarantee the biocompatibility of BDC-Mo [5]. However, BHET-Mo maintains the cell viability up to 48 h of incubation, this possibly obeys to the biocompatibility of ester bonding in this material as the XPS indicates [23].

As the fibroblast metabolism has a crucial role in skin tissue regeneration to obtain the wound closure in a minor lapse of time. This indicated that BDC-Mo and BHET-Mo metal-organic complexes possess suitable characteristics to be applied in biomedical applications such as tissue engineering, controlled delivery of drugs and antiproliferative agent against cancer cells [16].

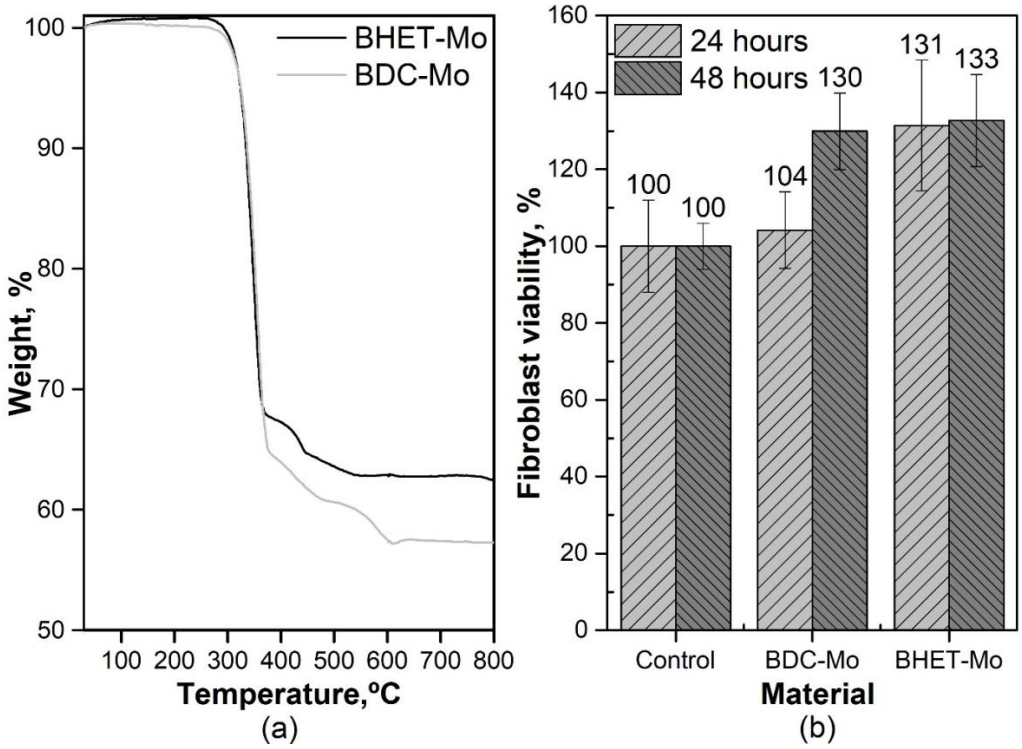

Fig.6. (a) Thermogravimetric analysis and (b) fibroblast viability of molybdenum complexes

4. Conclusion

The physicochemical characterization results indicated that molybdenum-based complexes are molybdate units bonded to BDC and BHET ligand by urea bonding obtaining rectangular prism particles made up of thin rods arrays typical of MoO_3 assemblies and molybdenum complexes, belonging to the monoclinic system with a P 2/m group space. The ATR-FTIR indicated that molybdenum is covalently coordinated to BDC and BHET ligands by their carbonyl groups due the shift of their typical vibration band to lower wavenumbers. Also, the absence of bands at around 3400 cm^{-1} related to terminal hydroxyl groups in BHET-Mo material indicated the loss of hydroxyl groups which was confirmed by XPS indicating an additional peak of O1s related to ester bonding.

The high fibroblast viability of BDC-Mo and BHET-Mo compared with the control was attributed to the end carboxyl groups of BDC, end ethoxy groups of BHET and urea bonding, however the best biocompatibility of BHET-Mo was associated to the additional ester bonding present in this material. The biocompatibility shown by molybdenum complexes indicated that these materials could be applied in tissue engineering devoted to healing skin, and controlled drug delivery.

Declarations

Source of Funding

This research was funded by Consejo Nacional de Ciencia y Tecnología (CONACyT) (grant FORDECYTPRO NACES/6660/2020).

Competing Interests Statement

The authors declare no competing financial, professional, and personal interests.

Ethical Approval

Based on institutional guidelines.

Consent for publication

Authors declare that they consented for the publication of this research work.

Availability of data and material

Authors are willing to share the data and material according to relevant needs.

Authors' Contributions

All authors equally contributed to data collection, research, and paper drafting.

References

[1] Hille, R. (2002). Molybdenum and tungsten in biology. Trends Biochem. Sci., 27(7): 360–367.

[2] Mendel, R.R. (2005). Molybdenum: biological activity and metabolism. Dalton Trans., 21: 3404–3409.

[3] Zu, Y., Yao, H., Wang, Y., Yan, L., Gu, Z., Chen, C., Gao, L & Yin, W. (2021). The age of bioinspired molybdenum-involved nanozymes: synthesis, catalytic mechanisms, and biomedical applications. View, 2(3): 20200188.

[4] Mendel, R.R. (2009). Cell biology of molybdenum. Biofactors, 35(5): 429–434.

[5] Pandey, A., Dhas, N., Deshmukh, P., Caro, C., Patil, P., García-Martín, M.L., Padya, B., Nikam, A., Mehta, T. & Mutalik, S. (2020). Heterogeneous surface architectured metal-organic frameworks for cancer therapy, imaging, and biosensing: a state of the art review. Coord. Chem. Rev., 409: 213212.

[6] Bhardwaj, N., Pandey, S.K., Mehta, J., Bhardwaj, S.K., Kim, K.H. & Deep. A. (2018). Bioactive nano-metal-organic frameworks as antimicrobial against Gram-positive and Gram-negative bacteria. Toxical. Res, 7(5): 931–941.

[7] Feng, M., Zhang, P., Zhou, H.C. & Sharma, V.K. (2018). Water-stable metal-organic frameworks for aqueous remvoal of heavy metals and radionuclides: A review. Chemosphere, 209: 783–800.

[8] Stoski, A., Viante, M.F., Santos Nunes, C., Curti Muñiz, E., Felsner, M.A. & Policiano Almeida, C.A. (2016). Water-stable metal-organic frameworks for aqueous remvoal of heavy metals and radionuclides: A review. Polym. Int., 65(9): 1024–1030.

[9] Cabrera-Munguia, D.A., León-Campos, M.I., Claudio-Rizo, J.A., Solis-Casados, D.A., Flores-Guia, T.E. & Cano-Salazar, L.F. (2021). Potential biomedical applications of a new MOF based on a derived PET: Synthesis and characterization. Bull. Mat. Sci., 44(4): 245.

[10] Cabrera-Munguia, D.A., Claudio-Rizo, J.A., Aguayo-Morales, H. & Martínez-Mora, E.I. (2022). Gel-based on collagen-polyacrylate-MOF as an adjuvant in skin wound healing: a case study. Asian Journal of Basic Science & Research, 4(1): 60–69.

[11] Saska, M. & Myerson, A.S. (1985). Polymorphism and aging in terephthalic acid. Crystal Res. & Technol., 20(2): 201–208.

[12] Castaño, V.M., Alvarez-Castillo, A., Vazquez-Polo, G., Acosta, D. & González, V. (1998). High resolution electron microscopy of bis-(2-hydroxyethyl) terephthalate crystalline polymers. Microsc. Res. Tech., 40: 41–48.

[13] Yang, L., Li, X., Qi, T., Liu, G., Peng, Z. & Zhou, Q (2020). Direct synthesis of pure ammonium molibdates from ammonium tetramolybdate and ammonium bicarbonate. ACS Sustainable Chem. Eng., 8(49): 18237–18244.

[14] Wang, M-L., Zhong, G-Q. & Chen, L. (2016). Synthesis, optical characterization, and thermal decomposition of complexes based on biuret ligand. Int. J. Opt., 16: 5471818.

[15] Hou, G-F., Wang, X-D., Yu, Y-H., Gao, J-S., Wen, B. & Yan, P-F. (2013). A new topology constructed from an octamolybdate and metallomacrocycle coordination complex. CrystEngComm., 15: 249–251.

[16] Joshi, A., Gupta, R., Sharma, D. & Singh M. (2021). Mo(VI) based coordination polymer as antiproliferative agent against cancer cells. Dalton Trans., 50: 1253–1260.

[17] Maheswari, N. & Muralidharan, G. (2017). Controlled synthesis of nanostructured molybdenum oxide electrodes for high performance supercapacitor devices. Appl. Surf. Sci., 416: 461–469.

[18] Cao, X., Zheng, B., Shi, W., Yang, J.., Fan, Z., Luo, Z., Rui, X., Chen, B., Yan, Q. & Zhang, H. (2015). Reduced graphene oxide-wrapped MoO_3 composites prepared by using metal-organic frameworks as precursor for all solid state flexible supercapacitors. Adv. Mater., 27(32): 4695–4701.

[19] Zhang, X., Li, D., Dong, C., Shi, J. & Xu, Y. (2019). The synergistic supercapacitive performance of Mo-MOF/PANI and its electrochemical impedance spectroscopy investigation. Mater. Today Commun., 21: 100711.

[20] Zhou, X., Lu, X., Wang, Q., Zhu, M. & Li, Z. (2012). Effective catalysis of poly(ethylene terephthalate) (PET) degradation by metallic acetate ionic liquids. Pure Appl. Chem., 84(3): 789–801.

[21] Chithambararaj, A, Bhagya Mathi, D., Rajeswari Yogamalar, N. & Chandra Bose, A. (2015). Structural evolution and phase transition of $[NH_4]_6Mo_7O_2.4H_2O$ to 2D layered MoO_{3-x}. Mater. Res. Express, 2: 055004.

[22] Begüm Elmas Kimyonok, A. & Mehmet Ulutürk (2016). Determination of the thermal decomposition products of terephthalic acid by using curie-point pyrolyzer. J. Energ. Mater., 34(2): 113–122.

[23] Undin, J., Finne-Wistrand & Albertsson, AN. (2016). Adjustable degradation properties and biocompatibility of amorphous and functional poly(ester-acrylate)-based materials. Biomacromolecules, 15: 2800–2807.